

Hierarchical mesoporous silica prepared from ethyl-cyanoethyl cellulose cholesteric liquid crystalline phase

Wen Wang · Ruigang Liu · Weili Liu · Junjun Tan ·
Wenyong Liu · Hongliang Kang · Yong Huang

Received: 24 November 2009 / Accepted: 12 May 2010 / Published online: 28 May 2010
© Springer Science+Business Media, LLC 2010

Abstract Porous silica with hierarchical structures was prepared from ethyl-cyanoethyl cellulose/poly(3-(methacryloyloxy)propyl-trimethoxysilane) (E-CE)C/P(MPTOS) composites with fixed cholesteric liquid crystalline (LC) phase. The scanning and transmission electron microscopy (SEM and TEM) and N₂ sorption measurements results indicate that the silica prepared from cholesteric LC composites is of hierarchical macro-, meso- and micro-porous structures, and the average pore size of the silica can be tailored by the content of the cholesteric LC phase in the (E-CE)C/P(MPTOS) composites. The resultant silicas have high specific surface area with the highest value of 837 m²/g at the pore volume of 0.83 cm³/g. This approach provides a new choice for the preparation of porous silica materials, especially from the templates that are not compatible with aqueous system.

Introduction

Mesoporous silica materials with controllable pore size and high surface areas have attracted much attention due to their versatile applications in catalysis [1], separation [2–4], delivery [5–9], and sensors [10–12]. In the past decades, sol–gel methods were mainly used to prepare various kinds of mesoporous silicas; due to that it is easy to address and reproduce ultra-fine structures of the templates [13–16], in which surfactants [16–18] and block copolymer [19–23], as well as biomolecules [24–27], viruses [28], bacteria [29, 30], and biological tissues [31, 32], with unique micro- and meso-structures, are generally used as the templates due to the ordered and size controllable meso-structures. Moreover, water is generally needed to hydrolyze silica precursor to form polysiloxanes by which to fix the mesostructures of the templates in sol–gel methods. Therefore, the organic candidates for template should be compatible with both the aqueous sol phase and the resultant solidified gel replica [27]. The usage of some template candidates that undissolved or cannot be dispersed in aqueous media is limited.

As one of the most abundant and renewable natural polymers, cellulose and most of its derivatives can form cholesteric liquid crystalline (LC) phase in certain solvents, which made them the unique, inexpensive, and environmentally friendly templates for organic/inorganic hybrid materials and porous materials with unique architectures. The mesoporous silica has been synthesized by sol–gel method using cellulose nanorods [33] and hydroxypropyl cellulose [27]. We have found that ethyl-cyanoethyl cellulose ((E-CE)C) forms cholesteric LC phase in solvents, such as dichloroacetic acid [34, 35], acetic acid (Ac), and acrylic acid (AA) [36–38]. The cholesteric LC superstructure in polymerizable solvents (e.g., AA) can be fixed

W. Wang · R. Liu (✉) · W. Liu · J. Tan · W. Liu · H. Kang · Y. Huang (✉)

State Key Laboratory of Polymer Physics and Chemistry,
Beijing National Laboratory for Molecular Sciences,
Institute of Chemistry, Chinese Academy of Sciences,
Beijing 100190, China
e-mail: rgliu@iccas.ac.cn

Y. Huang
e-mail: yhuang@mail.ipc.ac.cn

W. Wang · W. Liu · J. Tan · W. Liu
Graduate University of Chinese Academy of Sciences,
Beijing 100039, China

Y. Huang
National Engineering Research Center of Plastics,
Technical Institute of Physics and Chemistry,
Chinese Academy of Sciences, Beijing 100190, China

by photo-polymerization [36, 37] and used as an excellent template for the synthesis of mesoporous silica.

In this study, 3-(methacryloyloxy)propyl-trimethoxysilane (MPTOS), a photopolymerisable silica precursor, was introduced into the (E-CE)C/Ac cholesteric LC phase. The cholesteric LC superstructure was then fixed by photo-polymerization of MPTOS. The resultant fixed cholesteric LC phase was used as precursor for the synthesis of mesoporous silica, and the influence of the cholesteric LC phase on the morphology, pore structures, and absorption properties of the resultant porous silica was investigated.

Experimental section

Materials

Ethyl-cyanoethyl cellulose [(E-CE)C] ($M_n = 7 \times 10^4$ g/mol) was synthesized from ethyl cellulose (EC) (Luzhou Chemical Plant, China). The degree of substitution of ethyl and cyanoethyl groups is 2.1 and 0.32, respectively [35–37]. Acetic acid (chemical pure, Sinopharm Chemical Reagent Beijing Co.,Ltd., China) was dried with anhydrous MgSO₄ and distilled under reduced pressure at 50 °C before use. The crosslinker divinyl benzene (DVB) and the silica precursor MPTOS were purchased from Alfa Aesar and used directly without further purification. The photo initiator DAROCUR 1173 was purchased from Ciba Specialty Chemicals.

Preparation of (E-CE)C/MPTOS/Ac liquid crystals solution and (E-CE)C/P(MPTOS) films

Different ratio of MPTOS, Ac, initiator DAROCUR 1173 and crosslinker DVB were mixed together to form a clear MPTOS/Ac/1173/DVB solution. (E-CE)C/MPTOS/Ac cholesteric LC solutions were prepared by mixing (E-CE)C with the above-prepared solution at room temperature. The Mixtures were sealed in a test tube and stored in dark at room temperature for 2 weeks to obtain homogeneous solutions. The solutions were then sandwiched between two microscope slides, sealed with solid wax, and left in dark at room temperature for 8 h to eliminate the internal

stress. The solution films were then exposed under a UV source (250 W, $\lambda = 365$ nm) for 8 min, and the MPTOS in the cholesteric LC solution was photo-polymerized to form soft and slight ivory-white films with a thickness of about 1 mm. The distance between the UV source and the sample plane was 8 cm. In this procedure, the (E-CE)C cholesteric LC phase in the solution can be fixed by the P(MPTOS) network. Then the films were dried in vacuum at 40 °C for 24 h to eliminate the Ac. And then crisp and transparent ethyl-cyanoethyl cellulose/poly(3-(methacryloyloxy)propyl-trimethoxysilane) (E-CE)C/P(MPTOS) composite films were obtained. The weight content of the components of two series of samples with the same (E-CE)C content in the solution and the same content of P(MPTOS) in the (E-CE)C/P(MPTOS) composites is listed in Table 1.

Synthesis of silica hierarchical networks

The dried (E-CE)C/P(MPTOS) composite films were set in a tubular muffle furnace and preserved at 300 °C in N₂ gas for different time first, and then sintered in air flow at 550 °C for 12 h to eliminate the organic component completely. After cooling to room temperature, the white silica blocks or powders were taken out from the furnace.

Instruments and characterization

A polarized optical microscope (POM) (Olympus BH-2, Japan) equipped with a CCD camera was used to observe cholesteric LC texture of the films. The morphology of the freezing fractured surface of the dried (E-CE)C/P(MPTOS) cholesteric LC composite films was observed by scanning electron microscope (SEM) (JEOL JSM 6700F, Japan) at 10 kV. The microstructures of the sintered silica were observed by SEM at 10 kV after sticking on the carbon conductive tape, and by high resolution transmission electron microscope (TEM) (JEOL JEM 2200FS, Japan) at 200 kV after dispersion the powder in water and dropping on the microporous collodium-coated copper grids. Wide angle X-ray diffraction (WAXD) experiments were performed on an X-ray diffractometer (Bruker D8 Discover, Germany) at room temperature. Small angle X-ray scattering (SAXS) experiments were performed at beam line

Table 1 Details of the samples preparation

Samples	Ac (wt%)	MPTOS (wt%)	(E-CE)C (wt%)	P(MPTOS) in resultant composites (wt%)
A	55	0	45	0
B	49	6	45	12
C	44	11	45	20
D	41	14	45	24
E	37	18	45	29

4B9A of Beijing Synchrotron Radiation Facility (BSRF). The wavelength of the X-ray was 1.54 Å. The two-dimensional scattering data obtained were circularly averaged to transform one-dimensional scattering data and analyzed by subtracting the background noise. N₂ adsorption isotherms were measured using a Micromeritics ASAP 2020 analyzer at 77 K. Before measurements were taken, all samples were degassed at 473 K for 10 h. The specific surface area was calculated using the BET equation, using data in the P/P_0 region between 0.05 and 0.20. The BJH (Barret-Joyner-Halenda) method was applied to analyze the mesopore size distributions using the adsorption branch. Total pore volume was estimated from the amount of nitrogen adsorbed at a relative pressure of about 0.98.

Results and discussion

Sol-gel methods were mainly used to prepare various kinds of mesoporous silicas by using surfactants [16–18], block copolymer [19–23], biomolecules [24–27], etc. as the templates. In sol-gel methods, water is generally needed to hydrolyze silica precursor to form polysiloxanes by which to fix the mesostructures of the templates. In this study, we intend to prepare mesoporous silicas by using cholesteric LC phase in organic solvent as the template. In our previous study, it was found that cholesteric LC phase can be formed in (E-CE)C/Ac solutions in the (E-CE)C between 33 and 55 wt% [37]. It would be promising to prepare the mesoporous silicas by using these kinds of cholesteric LC phase as the template. Our previous study indicates that the cholesteric LC superstructure of the cellulosic lyotropic cholesteric LC phase can be fixed by using the polymerizable solvents (e.g., AA) [36, 37].

On the consideration of preparing mesoporous silicas, suitable silica precursors are needed. It was found that MPTOS would be one of the promising candidates due to that (E-CE)C can be dissolved in it. However, it was found

that no cholesteric LC phase can be formed in (E-CE)C/MPTOS solutions. Fortunately, cholesteric LC phase can be formed when (E-CE)C was dissolved in MPTOS/Ac mixed solvent as listed in Table 1. Meanwhile, the reflected light of the cholesteric LC phase changed from green to blue and then disappeared with the increase of MPTOS content in (E-CE)C/Ac/MPTOS solutions (top Fig. 1), which is attributed to the decrease of the helix pitch of the cholesteric LC phase in the solutions. When the silica precursor MPTOS in the cholesteric LC solutions was cross-linked by photo-polymerization and the solvent Ac was removed, (E-CE)C/P(MPTOS) cholesteric LC composite can be obtained. POM micrographs in Fig. 1 indicate that there are ordered structures in the resultant (E-CE)C/P(MPTOS) composites. And there are two strong diffraction peaks on the WAXD curves of the (E-CE)C/P(MPTOS) composites (Fig. 2). The diffraction peak at about $2\theta = 20^\circ$ attributes to the packing of (E-CE)C chains in the composites, while the diffraction peak at around $2\theta = 9^\circ$ ($d = 9.8 \text{ \AA}$) is the characteristic diffraction peak of the cholesteric LC phase [37]. Both POM and WAXD results indicate that the cholesteric LC phase is fixed in the (E-CE)C/P(MPTOS) composites. WAXD results further show that the integral area ratio of the diffraction peak at $2\theta = 9^\circ$ to that at $2\theta = 20^\circ$ decreases with increasing P(MPTOS) content, which suggests that the ordering degree of cholesteric LC phase in the composites decreases with the increase of P(MPTOS) content.

Figure 3 shows the SEM micrographs of the freezing fractured surface of the resultant (E-CE)C/P(MPTOS) composites. At low P(MPTOS) content, e.g., below 20 wt%, typical ordered layer structure of cholesteric LC phase can be observed (Fig. 3a and b), which indicates the less influence on the cholesteric LC phase with the presence of P(MPTOS). However, the distance between two layers decreases with the increase of P(MPTOS) content (Fig. 3c–e). It also indicates that the helix pitch of the cholesteric LC phase decreases with the increasing

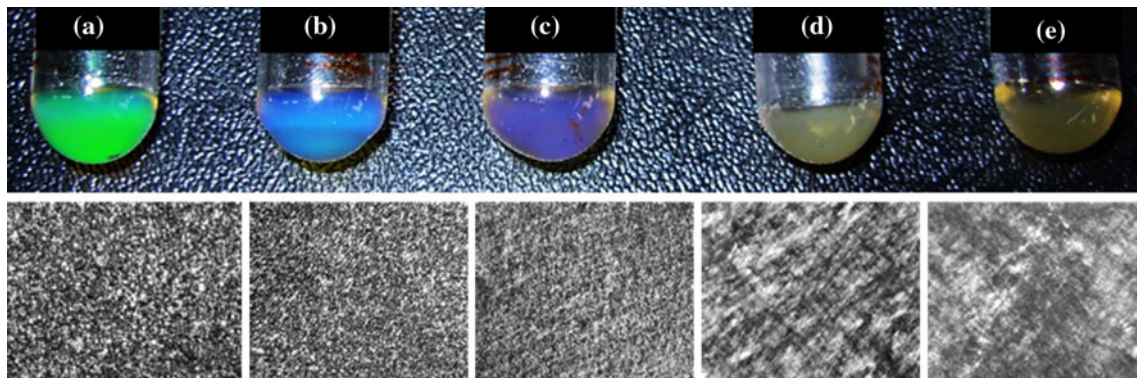


Fig. 1 Photographs (top) of the (E-CE)C/MPTOS/Ac cholesteric LC solutions and corresponding POM micrographs (bottom) of cholesteric LC films after photo-polymerization of MPTOS and removing Ac. The details of the sample preparation are listed in Table 1

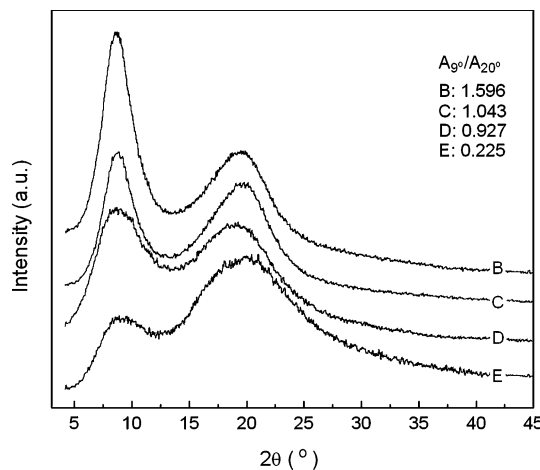


Fig. 2 WAXD curves of the (E-CE)C/P(MPTOS) cholesteric LC composite. Details of the samples preparation are listed in Table 1. A 9° /A 20° indicates the ratio of integral area of the diffraction peaks at $2\theta = 9^\circ$ and 20° for the corresponding samples

P(MPTOS) content, which is consisted with those light reflection color of the cholesteric solutions. And no ordered layer structure can be observed at the P(MPTOS) content of 29 wt%, which also indicates that the ordering degree of cholesteric LC phase in the composites decreases with the increase of P(MPTOS) content as shown in the WAXD results.

When the resultant (E-CE)C/P(MPTOS) composites were precalcined in N₂ atmosphere at 300 °C for 12 h and calcined in air atmosphere at 550 °C for 12 h, silica blocks

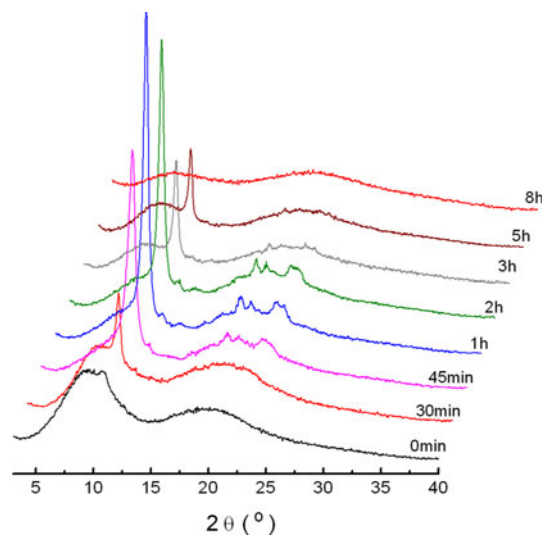


Fig. 4 Wide angle X-ray diffraction patterns of (E-CE)C/P(MPTOS) composite (Sample D in Table 1) at different times that precalcined in N₂ atmosphere

or powder can be obtained. Generally, powder form silica was obtained at the lowest content of P(MPTOS) in this study, say 12 wt% (Sample B as listed in Table 1), while block silicas were obtained in at higher P(MPTOS) content. During precalcined procedure, a diffraction peak at around $2\theta = 11^\circ$ appeared when the composites were precalcined for 30 min (Fig. 4). This peak is generally attributed to the silicone networks [39, 40]. The result indicates the hydrolysis and condensation occurred and silicone network

Fig. 3 The SEM micrographs of the freezing fractured surface of the (E-CE)C/P(MPTOS) composite. The details of the sample preparation are listed in Table 1. **a** B, **b** C, **c** D, and **d** E

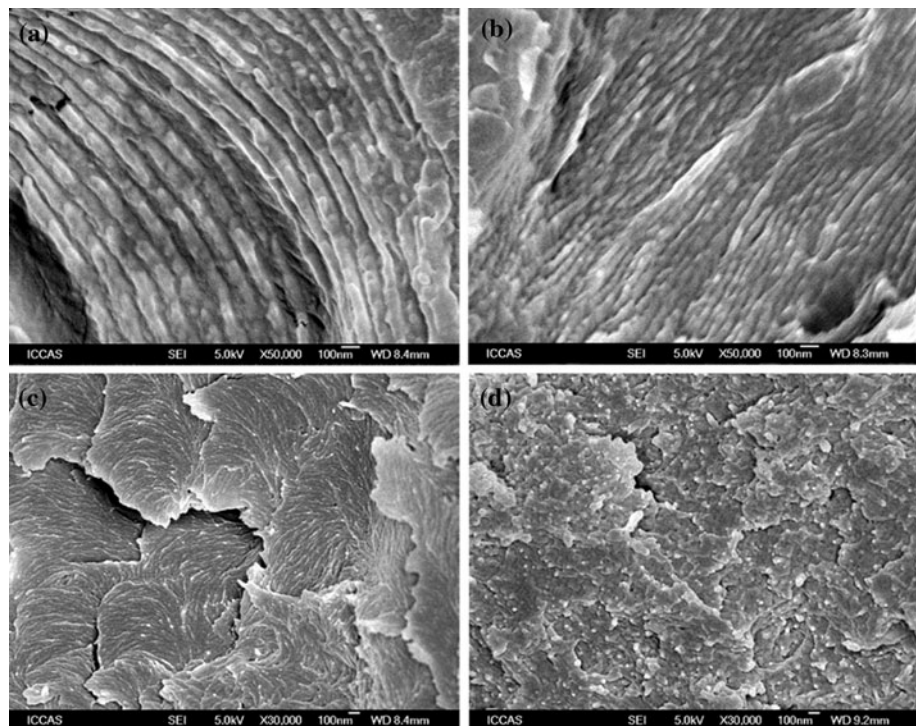
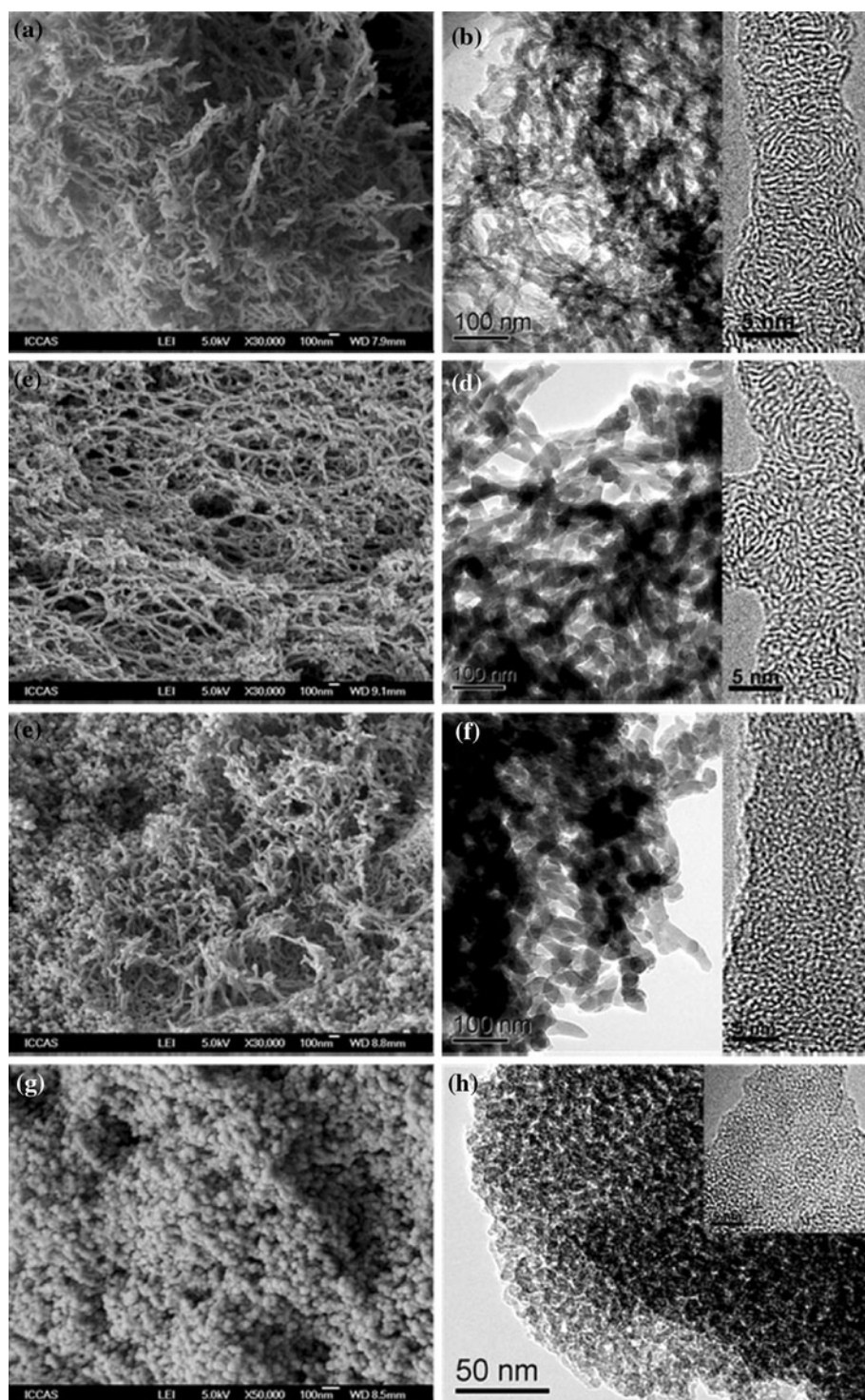


Fig. 5 The SEM and TEM micrographs of the silica sintered from samples B (a, b), C (c, d), D (e, f), and E (g, h)



formed during the pre-calcination procedure. Moreover, the diffraction peak of the silicone network became weak and disappeared after the composites were precalcined for 1 h and totally disappeared at 8 h (Fig. 4), which indicates the formation of amorphous silica precursors. The resultant silica materials were observed by using SEM and TEM (Fig. 5). When the P(MPTOS) content in the precursor

composites is below 20 wt%, corresponding to higher ordering degree of cholesteric LC structure in the (E-CE)/C/P(MPTOS) composites, the resultant sintered silica is composed of nanowires with diameter of 10–70 nm and length up to microns. Moreover, the nanowires connected with each other to form three-dimensional networks with macropores of 10–100 nm size (Fig. 5a–d). High-resolution

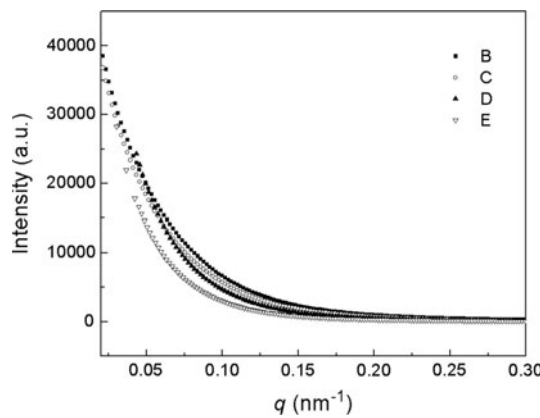


Fig. 6 SAXS curves of resultant silicas prepared from the samples listed in Table 1

TEM observation shows that there are small lamellar-like micropores in the silica nanowires with the diameter less than 20 nm (the right inserts of Fig. 5b and d). The inter-space between the two neighbored lamellar-like micropores is about 0.6–0.8 nm, which is associated with the d-space (9.8 Å) of the (E-CE)C molecules lamellar structure in cholesteric LC phase. When P(MPTOS) content in the precursor composites was increased to 24 wt% and part of the cholesteric LC phase in the precursor composite will be destroyed, the resultant sintered silica is composed of both nanorods and nanoparticles as shown in Fig. 5e and f. Meanwhile, no small lamellar-like micropores can be observed by high resolution TEM micrograph (right insert of Fig. 5f). Further increase of the P(MPTOS) content in the precursor composites up to 29 wt% and the cholesteric LC phase in the precursor is less ordered, the resultant silica are composed of fused nanoparticles with the diameter of 10–50 nm (Fig. 5g and h). And no lamellar-like micropores can be observed (Fig. 5h). The results indicate that hierarchical macro- and micro-pores can be formed in the resultant silica from the cholesteric LC precursor composites. However, small angle X-ray scattering results show that there is no ordered structure in all the resultant silicas (Fig. 6). The lamellar-like micropores in the silica nanowires (the right inserts of Fig. 5b and d) are not real ordered structure. The micro-pores arranged randomly in the resultant silicas.

The porosity of the silica was characterized by nitrogen sorption measurements, and the results are shown in Fig. 7a. The specific surface area, average pore size, and specific pore volume of the silicas prepared from the cholesteric LC composites with different P(MPTOS) contents are listed in Table 2. The results show that the average pore size decreases with the increasing P(MPTOS) content in the precursor composites. The resultant silica from the precursor composites with higher ordered cholesteric LC phase has a broad distributed pore size in the range 5–60 nm (samples B and C) compared to those

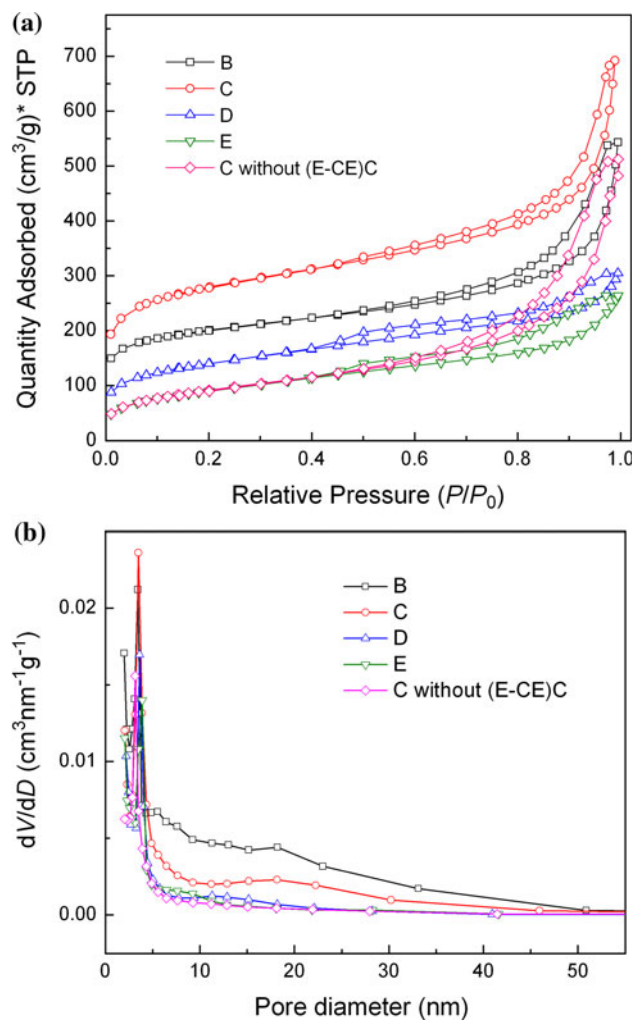


Fig. 7 The isotherm N_2 adsorption–desorption curves (a) and the pore size distribution (b) of the porous silica prepared from the precursors as listed in Table 1. The silica prepared from a sample without (E-CE)C is presented for comparison

silicas prepared from the precursor composites with less ordered cholesteric LC phase (samples D and E) (Fig. 7b). The results indicate that the cholesteric LC phase plays a key role on the formation of mesopores and macropores in the resultant silica. The specific surface area of the silica sintered from samples B and C is obviously higher than that of samples D and E. The larger average pore size and the higher specific surface area are due to the macropores twisted with nanowires and layered micropores in the nanowires as shown by the SEM and TEM observation (Fig. 5).

Conclusion

We have demonstrated a novel template-directed route to prepare porous silica with hierarchical structures from

Table 2 Quantitative adsorption data of the resultant mesoporous silicas

Samples	BET surface area (m ² /g)	BJH average pore diameter (nm)	Adsorption pore volume (cm ³ /g)
B	628	9.5	0.66
C	837	8.2	0.83
D	495	7.3	0.59
E	328	4.8	0.40
C without (E-CE)C	335	3.4	0.42

(E-CE)C/P(MPTOS) composites with fixed cholesteric LC phase through photopolymerization and thermal treatment in nonaqueous system. The SEM, TEM, and N₂ sorption measurements results indicate that the silica prepared from cholesteric LC composites is of hierarchical macro-, meso-, and micro-porosity, and the average pore size of the silica can be tailored by the content of the cholesteric LC phase in the (E-CE)C/P(MPTOS) composites. The highest specific surface area of the resultant silicas is 837 m²/g at the pore volume of 0.83 cm³/g. This approach provides a new choice for the preparation of porous silica materials, especially from the templates that are not compatible with aqueous system.

Acknowledgements Financial supports of National Natural Scientific Foundation of China (NNSFC) (Grant No. 50821062) and the Project of Knowledge Innovation Program of Chinese Academy of Sciences are gratefully acknowledged.

References

- Huh S, Chen HT, Wiench JW, Pruski M, Lin VSY (2005) Angew Chem Int Ed 44:1826
- Mattigod SV, Feng XD, Fryxell GE, Liu J, Gong ML (1999) Sep Sci Technol 34:2329
- Newalkar BL, Choudary NV, Kumar P, Komarneni S, Bhat TSG (2002) Chem Mater 14:304
- Gabashvili A, Medina DD, Gedanken A, Mastai Y (2007) J Phys Chem B 111:11105
- Giri S, Trewyn BG, Stellmaker MP, Lin VSY (2005) Angew Chem Int Ed 44:5038
- Yang Q, Wang SH, Fan PW et al (2005) Chem Mater 17:5999
- Kim J, Lee JE, Lee J et al (2006) J Am Chem Soc 128:688
- Slowing II, Trewyn BG, Giri S, Lin VSY (2007) Adv Funct Mater 17:1225
- de Sousa A, Maria DA, de Sousa RG, de Sousa EMB (2010) J Mater Sci 45:1478. doi:[10.1007/s10853-009-4106-3](https://doi.org/10.1007/s10853-009-4106-3)
- Yantasee W, Lin YH, Li XH, Fryxell GE, Zemanian TS, Viswanathan VV (2003) Analyst 128:899
- Balaji T, Sasidharan M, Matsunaga H (2005) Analyst 130:1162
- Goettmann F, Moores A, Boissiere C, Le Floch P, Sanchez C (2005) Small 1:636
- Soler-illia GJD, Sanchez C, Lebeau B, Patarin J (2002) Chem Rev 102:4093
- Jung JH, Ono Y, Hanabusa K, Shinkai S (2000) J Am Chem Soc 122:5008
- Che S, Liu Z, Ohsuna T, Sakamoto K, Terasaki O, Tatsumi T (2004) Nature 429:281
- Huo QS, Margolese DI, Stucky GD (1996) Chem Mater 8:1147
- Kresge CT, Leonowicz ME, Roth WJ, Vartuli JC, Beck JS (1992) Nature 359:710
- Tanev PT, Pinnavaia TJ (1995) Science 267:865
- Chen A, Komura M, Kamata K, Iyoda T (2008) Adv Mater 20:763
- Goltner CG, Henke S, Weissenberger MC, Antonietti M (1998) Angew Chem Int Ed 37:613
- Zhao DY, Feng JL, Huo QS et al (1998) Science 279:548
- Tirumala VR, Pai RA, Agarwal S et al (2007) Chem Mater 19:5868
- Niu DC, Li YS, Dong WJ, Zhao WR, Li L, Shi JL (2009) J Mater Sci 44:6519. doi:[10.1007/s10853-009-3675-5](https://doi.org/10.1007/s10853-009-3675-5)
- Han BH, Antonietti M (2002) Chem Mater 14:3477
- Kessel S, Thomas A, Borner HG (2007) Angew Chem Int Ed 46:9023
- Polarz S, Smarsly B, Bronstein L, Antonietti M (2001) Angew Chem Int Ed 40:4417
- Thomas A, Antonietti M (2003) Adv Funct Mater 13:763
- Fowler CE, Shenton W, Stubbs G, Mann S (2001) Adv Mater 13:1266
- Davis SA, Burkett SL, Mendelson NH, Mann S (1997) Nature 385:420
- Livage J, Coradin T, Roux C (2001) J Phys-Condens Mat 13:R673
- Valtchev VP, Smahi M, Faust AC, Vidal L (2004) Chem Mater 16:1350
- Sapei L, Noeske R, Strauch P, Paris O (2008) Chem Mater 20:2020
- Dujardin E, Blaseby M, Mann S (2003) J Mater Chem 13:696
- Wang LG, Huang Y (2001) Liq Cryst 28:1673
- Wang LG, Huang Y (2002) Macromolecules 35:3111
- Wang LG, Huang Y (2000) Macromolecules 33:7062
- Wang LG, Huang Y (2004) Macromolecules 37:303
- Huang Y, Jiang SH (1992) Polym Bull 27:535
- Liu L, Tian M, Zhang W, Zhang L, Mark JE (2007) Polymer 48:3201
- Ohlberg SM, Alexander LE, Warrick EL (1958) J Polym Sci 27:1